Proteomic Analysis of Laser-Captured Paraffin-Embedded Tissues: A Molecular Portrait of Head and Neck Cancer Progression

Vyomesh Patel,[1] Brian L. Hood,[2] Alfredo A. Molinolo,[1] Norman H. Lee,[4] Thomas P. Conrads,[2] John C. Braisted,[5] David B. Krizman,[3] Timothy D. Veenstra,[2] and J. Silvio Gutkind[1]

Abstract

Purpose: Squamous cell carcinoma of the head and neck (HNSCC), the sixth most prevalent cancer among men worldwide, is associated with poor prognosis, which has improved only marginally over the past three decades. A proteomic analysis of HNSCC lesions may help identify novel molecular targets for the early detection, prevention, and treatment of HNSCC.

Experimental Design: Laser capture microdissection was combined with recently developed techniques for protein extraction from formalin-fixed paraffin-embedded (FFPE) tissues and a novel proteomics platform. Approximately 20,000 cells procured from FFPE tissue sections of normal oral epithelium and well, moderately, and poorly differentiated HNSCC were processed for mass spectrometry and bioinformatic analysis.

Results: A large number of proteins expressed in normal oral epithelium and HNSCC, including cytokeratins, intermediate filaments, differentiation markers, and proteins involved in stem cell maintenance, signal transduction, migration, cell cycle regulation, growth and angiogenesis, matrix degradation, and proteins with tumor suppressive and oncogenic potential, were readily detected. Of interest, the relative expression of many of these molecules followed a distinct pattern in normal squamous epithelia and well, moderately, and poorly differentiated HNSCC tumor tissues. Representative proteins were further validated using immunohistochemical studies in HNSCC tissue sections and tissue microarrays.

Conclusions: The ability to combine laser capture microdissection and in-depth proteomic analysis of FFPE tissues provided a wealth of information regarding the nature of the proteins expressed in normal squamous epithelium and during HNSCC progression, which may allow the development of novel biomarkers of diagnostic and prognostic value and the identification of novel targets for therapeutic intervention in HNSCC.

Authors' Affiliations: [1]Oral and Pharyngeal Cancer Branch, National Institute of Craniofacial and Dental Research, NIH, Bethesda, Maryland; [2]Laboratory of Proteomics and Analytical Technologies, Science Applications International Corporation-Frederick, Inc., National Cancer Institute, Frederick, Maryland; [3]Expression Pathology Incorporated, Gaithersburg, Maryland; [4]Department of Pharmacology and Physiology, The George Washington University Medical Center, Washington, District of Columbia; and [5]Pathogen Functional Genomics Resource Center, J. Craig Venter Institute, Rockville, Maryland

Received 6/8/07; revised 10/19/07; accepted 12/5/07.

Grant support: Intramural Program, National Institute of Dental and Craniofacial Research and National Cancer Institute, NIH, under contract NO1-CO-12400.

The costs of publication of this article were defrayed in part by the payment of page charges. This article must therefore be hereby marked *advertisement* in accordance with 18 U.S.C. Section 1734 solely to indicate this fact.

Note: Supplementary data for this article are available at Clinical Cancer Research Online (http://clincancerres.aacrjournals.org/).

The content of this publication does not necessarily reflect the views or policies of the Department of Health and Human Services, nor does mention of trade names, commercial products, or organization imply endorsement by the U.S. Government.

Current address for B.L. Hood and T.P. Conrads: Clinical Proteomics Facility, University of Pittsburgh Cancer Institute, Pittsburgh, Pennsylvania.

Requests for reprints: J. Silvio Gutkind, Oral and Pharyngeal Cancer Branch, National Institute of Dental and Craniofacial Research, NIH, 30 Convent Drive, Building 30, Room 211, Bethesda, MD 20892-4330. Phone: 301-496-6259; Fax: 301-402-0823; E-mail: sg39v@nih.gov.

doi:10.1158/1078-0432.CCR-07-1497

Head and neck squamous cell carcinoma (HNSCC) is the sixth most frequent cancer in the United States and the fourth most prevalent cancer among men worldwide (1). The prognosis of HNSCC patients is relatively poor, largely due to the advanced nature of the disease at the time of diagnosis. The identification of the molecular mechanisms underlying HNSCC initiation and progression could aid in the development of new diagnostic and treatment options for this disease (2, 3). In this regard, analysis of mRNA transcripts using high-throughput gene array analysis has helped identify numerous molecules that may contribute to cancer development (reviewed in ref. 4). A shortcoming of this approach, however, stems from the discordance between transcript levels and protein abundance in a highly complex and readily changing disease microenvironment such as cancer (5). A proteomic analysis is urgently needed, as it allows the comprehensive assessment of the distinct molecular profile of each cancer type, thus affording the opportunity of identifying novel prognostic markers and therapeutic targets (6).

Improved protein extraction protocols (7) combined with recently developed mass spectrometry (MS) techniques and fully annotated genomic databases has allowed the identification of trace amounts of proteins present in complex samples (8).

Table 1. Clinical features of HNSCC cases and summary of the liquid chromatography–tandem MS data

Sample	Pathology	Sex	Age	Location	Total peptides	Unique proteins	Total (n = 4)
2N	N	M	71	Oral	1,143	207	
8N	N	U	50	Oral	775	140	
36N	N	M	63	Oral	620	137	
37N	N	M	55	Oral	339	106	391
12A	WD SCC	F	62	Oral	1,454	376	
14A	WD SCC	F	U	Oral	1,570	356	
15A	WD SCC	F	60	Oral	1,586	351	
16A	WD SCC	F	42	Oral	1,721	323	866
1A	MD SCC	F	67	Oral	1,833	366	
2A	MD SCC	M	56	Oral	1,422	322	
6A	MD SCC	M	U	Oral	838	216	
9A	MD SCC	M	33	Oral	795	194	729
10A	PD SCC	F	52	Oral	1,202	239	
11A	PD SCC	M	72	Oral	1,411	296	
13A	PD SCC	U	50	Oral	1,073	257	
18A	PD SCC	U	U	Oral	774	185	676

NOTE: All clinical samples were retrieved from the Head and Neck Tissue Microarray initiative, and chosen based primarily on location within the oral cavity. Samples were assessed for the presence of normal and malignant squamous epithelia that were either WD, MD, or PD. Where available, information on patient gender and age is included. Summary of number of peptides and proteins detected in each sample is included. Abbreviations: N, normal; M, male; F, female; U, unknown.

Furthermore, the combination of proteomic analysis with laser capture microdissection may afford performing the proteomic characterization of normal and pathologic cell populations from clinical specimens, thus reflecting their protein make up as they exist *in vivo* (9). We have recently conducted the first proteome-wide analysis of microdissected frozen HNSCC tissue (10). Although protein recovery was acceptable, challenges related to the poor histology and limited availability of appropriately preserved frozen tissue samples still remain.

Formalin fixation and tissue embedding in paraffin wax (FFPE) is a universal approach for tissue processing, histologic evaluation, and routine diagnosis, as it preserves the cellular morphology and tissue architecture. FFPE clinical specimens, however, are not routinely used for MS-based proteomic studies because formaldehyde-induced cross-linking renders proteins relatively insoluble and unsuitable for extraction and subsequent MS analysis (11). In this study, we combined the use of laser capture microdissection, newly developed procedures enabling the extraction of peptides directly from FFPE samples, and optimized chromatographic approaches to undertake a large-scale proteomic study to identify proteins expressed in FFPE HNSCC tissues. We show that this novel proteomics platform enables the identification of hundreds of proteins expressed in normal oral epithelium and cancerous HNSCC lesions. A large number of differentiation markers, stem cell proteins, and molecules that are likely to play key roles in aberrant cell growth, including proteins involved in cell cycle control, angiogenesis, and metastasis, were identified. These proteins may represent novel biomarkers with diagnostic and prognostic value for HNSCC, as well as new potential molecular targets for pharmacologic intervention in this disease.

Materials and Methods

Tissues. Appropriate paraffin blocks of formalin-fixed tissues from normal squamous epithelium (n = 4), and well differentiated (WD; n = 4), moderately differentiated (MD; n = 4), and poorly differentiated (PD; n = 4) HNSCC were retrieved from the Head and Neck Cancer Tissue Array Repository (TMA)[6] (12), under an approved Research Activity Involving Human Subjects protocol, from the Office of Human Subjects Research, NIH, involving the use of anonymous normal and HNSCC tissues. Before analysis, H&E-stained section from each sample was evaluated and the suitability of inclusion for the study was determined. Five-micrometer sections were used for all subsequent analysis.

Immunohistochemistry. Primary antibodies used for validation studies include mouse anti–desmoglein-3 (Invitrogen; 1:25), rabbit anti-cytokeratin 4 (Abcam; 1:100), mouse anti-cytokeratin 16 (Abcam; 1:25), rabbit anti-desmoplakin antibody (Abcam; 1:200), and mouse anti-vimentin (Dako; 1:100). Secondary antibodies conjugated with biotin (Vector) were used, diluted to 1:400. Tissue slides containing archival FFPE sections, or tissue microarrays (TMA)[6] consisting of 508 HNSCC and controls, were processed for immunohistochemical analysis as described in Supplementary Material.

Laser capture microdissection and protein extraction. FFPE oral cancer tissue sections were deparaffinized in SafeClear II, hydrated, and stained in Mayer's hematoxylin followed by dehydration as described in Supplementary Material. For laser capture microdissection, stained uncovered slides were air dried and ~20,000 cells were captured onto CapSure LCM Caps (MDS Analytical Technologies) using a PIXCELL IIe microdissection equipment (MDS Analytical Technologies). Caps were transferred to a 0.5 mL sterile Eppendorf tube for protein extraction using the Liquid Tissue MS Protein Prep kit according to the manufacturer's protocol (Expression Pathology, Inc.), as described in Supplementary Material.

Tandem MS and bioinformatic analysis. FFPE-extracted samples were processed, quantified, and used for nanoflow reversed-phase liquid chromatography followed by tandem MS, as described in Supplementary Material. The spectra were searched against the UniProt human protein database (06/2005 release) from the European Bioinformatics Institute[7] using SEQUEST (Thermo Electron). Results were further filtered using software developed in-house to determine unique peptides and proteins, which has a predicted error <1.5% (13).

[6] http://www.nidcr.nih.gov/Research/ResearchResources/HeadandNeckTissueArrayInitiative.htm

[7] http://www.ebi.ac.uk/integr8

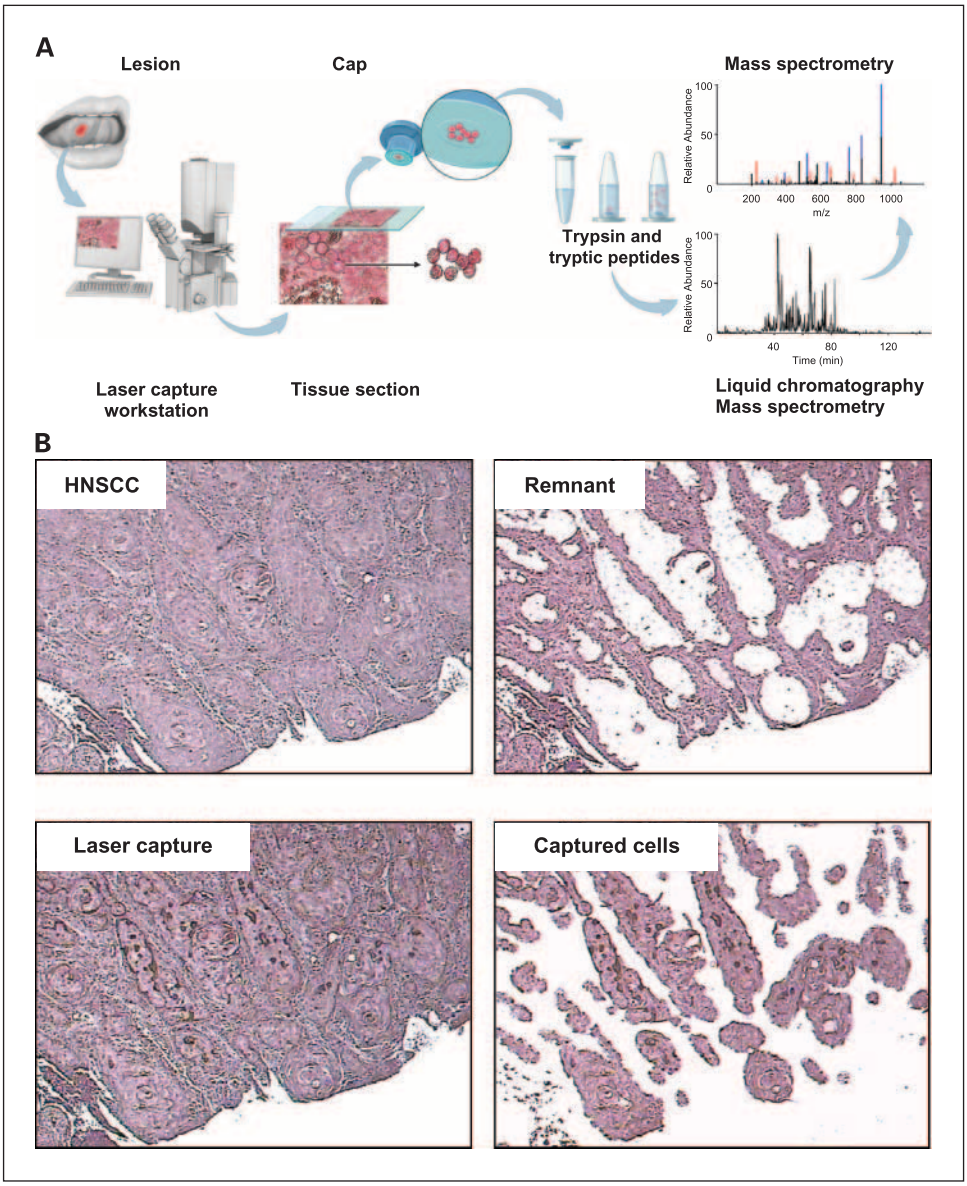

Fig. 1. Work flow for protein analysis of FFPE oral squamous cell carcinoma. *A,* different steps involved in the process of protein analysis from laser-captured FFPE cancer tissues, including (from *left* to *right*) tissue biopsy, laser capture microdissection, sample preparation, and analysis by reversed-phase liquid chromatography – tandem MS. The latter involves the initial separation of complex peptide mixtures by Nanoflow reversed-phase liquid chromatography, followed by LIT MS. A complex base peak chromatogram of a representative HNSCC case is included, as well as the tandem MS spectra of a selected peptide whose identity was confirmed as vimentin. *B,* laser capture microdissection of a WD FFPE oral squamous cell carcinoma (*top left*). The area of interest is pulsed with laser (*bottom left*) and captured cells were retrieved on a cap (*bottom right*). Remnant tissue remains on the slide (*top right*).

To facilitate the biological interpretation of the extensive protein lists generated in these studies, the protein accession numbers were used to classify the proteins in Gene Ontology categories, based on their biological process and molecular and cellular functions (14), and to perform Expression Analysis Systematic Explorer analysis,[8] which enables the discovery of enriched biological themes within gene/protein lists, and the generation of protein annotation tables.

Results

HNSCC samples and laser capture microdissection. To gain insight into the nature of proteins expressed during HNSCC progression, we conducted a proteomic analysis of FFPE HNSCC tumors arising within the oral cavity. Tissue samples were classified using light microscopic examination of H&E-stained sections into normal (i.e., oral stratified epithelia lacking malignant features) or squamous carcinomas that were WD, MD, or PD. Each group consisted of four independent samples. The available clinical information is included in Table 1. The analytic workflow for the overall study is depicted in Fig. 1, which is the result of combining two different technology platforms, laser capture microdissection, and tandem MS. As shown schematically (Fig. 1A) and in detail (Fig. 1B), laser capture microdissection is well suited for the rapid procurement of specific cell populations, which are captured onto caps for immediate processing and analysis. The complexity of the resulting peptide mixture extracted from each sample is exemplified in Fig. 1A by the base peak spectrum of a representative WD HNSCC tumor (*right*). A tandem MS spectrum identifying a peptide originating from vimentin is also shown in this figure. This proteomic platform results in broad dynamic range of peptide measurements, which may aid in the identification of important molecules involved in squamous carcinogenesis as well as biomarkers for HNSCC progression.

[8] http://david.abcc.ncifcrf.gov

Protein abundance in normal and tumor HNSCC. Samples containing ~20,000 cells were processed as described in Materials and Methods and analyzed using gas phase fractionation in the m/z dimension ($GPF_{m/z}$). To enable the comparison of protein expression across all tissue samples, we used a spectral count method in which each protein that was identified in any one set was evaluated based on the number of unique peptides identified, and the total number of times that those peptides were observed in five successive runs for each set (Table 1). The number of proteins identified for each set as a group (all four sample results pooled together) ranged from 391 in the normal oral epithelia to 866 total proteins in the WD HNSCC tumors.

The data sets for each group of clinical samples were sorted based on the number of peptides identified in all tissues combined and the percentage of these total peptides detected in normal and each of the classified HNSCC tissues. Those proteins detected in normal and all HNSCC tissues are listed in Table 2 and sorted based on the number of identified peptides. As indicated, 115 proteins were identified as shared across all normal and tumor tissues. The utility of this overall approach is reflected in the identification of 49 peptides for glyceraldehyde-3-phosphate dehydrogenase, a protein product of a housekeeping gene routinely used to normalize gene expression experiments. In spite of observing fewer overall peptides in normal oral epithelia, which may have resulted from a reduced protein recovery from these samples, the relative detection level of glyceraldehyde-3-phosphate dehydrogenase was nearly equal across all tissue groups analyzed in this study. Thus, it is also possible that normal tissues might exhibit a greater diversity of molecules, therefore fewer achieving the lowest limit of detection of our current analytic method.

Two groups of proteins, cytokeratins and desmosomal proteins, stood out as the most abundant in all four-tissue sets. With few notable exceptions, most keratins were nearly equally represented across all tissue samples. For example, cytokeratin 5, a keratin expressed in basal layer of normal stratified epithelia, was the most abundant and was identified by a similar number of peptides in each tissue group. Cytokeratin 14, another basal keratin, was less abundant in normal tissues. Conversely, cytokeratin 4, which is expressed in the nonkeratinazing layer of stratified epithelium, was more abundant in the normal samples. Desmosomal proteins, including desmoplakin, plakophilin 1, periplakin, and desmoglein precursors, were prominent in all samples. Also notable in this list were the family of calcium-binding proteins (calgranulin A, calgranulin B, S100 A14, calmodulin-like protein), keratinocyte differentiation markers (involucrin, small proline-rich protein 3, profilin 1, cornifin A, cornifin B), and many membrane-related molecules (Annexin A1, actin-like protein 2). A number of proteins including heat shock protein 27 (HSP27) (15), HSP70 (16), and glutathione *S*-transferase (15), expected to be of higher abundance in tumor samples, were identified. A number of signaling molecules (e.g., Ras GTPase-activating-like protein IQGAP1, obscurin, tyrosine-protein kinase ITK) were also identified. Conversely, the DNA excision repair protein ERCC-5 was found to be less abundant in tumor samples. These data indicate that the analysis of FFPE tissues enables the identification of a broad range of functionally diverse proteins in normal and tumor squamous epithelia, albeit many exhibit a distinct expression profile.

Proteins detected only in HNSCC. Having identified common proteins in both normal and tumor samples, a list of molecules only identified in tumor samples was collated (Table 3). Forty-two proteins unique to HNSCC were readily detected by multiple peptides (>10). Among them, the most abundant was vimentin, a protein involved in epithelial-mesenchymal transition. A variety of proteins involved in cell migration, signaling, and proteolysis were also identified. Eighty-five less abundant proteins (i.e., identified by >4 peptides but <10 peptides) across all tumor samples were also detected. This group included proteins involved in DNA synthesis, metabolism, and cell signaling. These data provide a list of proteins that may play a putative role in tumor progression.

Proteins detected in normal oral squamous epithelium. To gain insight into the proteins identified exclusively in normal samples, the initial data set was sorted to filter out molecules not found within the tumors, in descending order based on peptide numbers (Supplementary Table S1). The proteins in this list were identified by fewer peptides, reflecting their lower abundance in normal oral squamous epithelium. Interestingly, proteins identified by ≥3 unique peptides included the low-density lipoprotein receptor-related protein 12 precursor, also known as suppressor of tumorigenicity protein 7, and two particular proteins identified with a single peptide included, activin β B chain and adenomatous polyposis coli protein. The data indicate that a subset of proteins are expressed preferentially in normal tissues, indicating that they could play a role in any of the biological functions done by normal stratified oral epithelium, including maintenance of normal differentiation program and tumor suppression.

Proteins detected in differentiated tumor tissues. Proteins of interest detected exclusively in the WD tumors, albeit with few peptides, included those involved in the dynamic function of the cytoskeleton, as well as molecules stimulating the Notch pathway, such as Delta 4 and Delta 1 (Supplementary Table S2). Proteins of interest and detected only in the MD group with one peptide include Wilms' tumor-associated protein and esophageal cancer–related gene-coding leucine-zipper motif, and unusual cadherins and desmosomal proteins for epithelial cells such as placental cadherin and protocadherin γ A6 (Supplementary Table S3). Interesting proteins detected only the PD group include the potential oncoprotein AF1q (17), two peptides derived from epithelial protein lost in neoplasm, and numerous proteins involved in cell cycle control and fatty acid metabolism and membrane trafficking (Supplementary Table S4).

Comparisons of proteins between samples. The list of proteins identified in each group was also compared to explore whether they could increase our understanding of HNSCC pathogenesis and its progression. Proteins identified only in normal and WD tumors by ≥3 peptides included the stem cell protein PIWIL3 (ref. 18; Table 4; Supplementary Table S5). A number of proteins were common to WD and MD tumors, represented by oncoprotein DJ-1 (Supplementary Table S6). Similarly, common proteins between MD and PD tumors included the tumor promigratory protein JWA. Notably, low-abundance proteins shared by the same group of HNSCC tumors also included signal transducer and activator of transcription 3, its activating kinase, Janus-activated kinase 2, and the key translational regulating protein mammalian target of rapamycin (Supplementary Table S7), which are implicated in HNSCC progression

Table 2. Proteins identified in both normal and tumor HNSCC tissues

Accession	Protein	Peptides (number)	Normal (%)	WD (%)	MD (%)	PD (%)
P13647	Keratin, type II cytoskeletal 5 (cytokeratin 5; K5)	681	21.73	31.42	23.64	23.20
P02533	Keratin, type I cytoskeletal 14 (cytokeratin 14; K14)	449	7.80	42.54	29.18	20.49
P08779	Keratin, type I cytoskeletal 16 (cytokeratin 16; K16)	387	8.27	41.09	30.23	20.41
P15924	Desmoplakin (DP; 250/210 kDa paraneoplastic pemphigus antigen)	385	15.32	43.90	18.44	22.34
P19013	Keratin, type II cytoskeletal 4 (cytokeratin 4; K4)	179	77.65	3.91	12.29	6.15
P04264	Keratin, type II cytoskeletal 1 (cytokeratin 1; K1)	146	18.49	22.60	28.77	30.14
P14618	Pyruvate kinase, isozymes M1/M2 (CTHBP; THBP1)	136	13.24	40.44	25.74	20.59
P04083	Annexin A1 (Annexin I; lipocortin I; calpactin II)	120	21.67	35.00	20.83	22.50
Q13835	Plakophilin 1 (band-6-protein, B6P)	95	16.84	30.53	21.05	31.58
P06702	Calgranulin B (S100 calcium-binding protein A9)	87	24.14	37.93	19.54	18.39
P04792	Heat-shock protein β-1 (HspB1; heat shock 27 kDa protein; HSP 27)	83	4.82	28.92	31.33	34.94
P37802	Transgelin-2 (SM22-α homologue)	77	9.09	25.97	33.77	31.17
Q04695	Keratin, type I cytoskeletal 17 (cytokeratin 17; K17)	76	6.58	40.79	31.58	21.05
P60174	Triosephosphate isomerase (EC 5.3.1.1; TIM; triose-phosphate isomerase)	76	7.89	35.53	22.37	34.21
P12111	Collagen α 3(VI) chain precursor	69	2.90	31.88	46.38	18.84
P06576	ATP synthase β chain, mitochondrial precursor	67	5.97	32.84	32.84	28.36
P32926	Desmoglein 3 precursor (130 kDa pemphigus vulgaris antigen; PVA)	65	15.38	29.23	30.77	24.62
P19971	Thymidine phosphorylase precursor (PD-ECGF)	58	1.72	50.00	34.48	13.79
P07476	Involucrin	57	8.77	56.14	26.32	8.77
P19012	Keratin, type I cytoskeletal 15 (cytokeratin 15; K15)	54	37.04	9.26	18.52	35.19
P02545	Lamin A/C (70 kDa lamin)	49	4.08	34.69	32.65	28.57
P04406	Glyceraldehyde-3-phosphate dehydrogenase, liver (GAPDH)	49	22.45	24.49	20.41	32.65
Q9UBC9	Small proline-rich protein 3 (cornifin β; esophagin; 22 kDa pancornulin)	49	61.22	4.08	6.12	28.57
P61978	Heterogeneous nuclear ribonucleoprotein K (hnRNP K)	48	10.42	29.17	27.08	33.33
P35527	Keratin, type I cytoskeletal 9 (cytokeratin 9; K9)	46	21.74	23.91	8.70	45.65
P62263	40S ribosomal protein S14 (PRO2640)	44	2.27	29.55	45.45	22.73
P27482	Calmodulin-related protein NB-1 (calmodulin-like protein; CLP)	43	6.98	41.86	30.23	20.93
P10809	60 kDa heat shock protein, mitochondrial precursor (Hsp60)	42	14.29	33.33	11.90	40.48
P35908	Keratin, type II cytoskeletal 2 epidermal (cytokeratin 2e; K2e)	39	30.77	17.95	2.56	48.72
P02462	Collagen α 1(IV) chain precursor	38	34.21	21.05	26.32	18.42
P55072	Transitional endoplasmic reticulum ATPase (TER ATPase)	37	2.70	51.35	32.43	13.51
P30101	Protein disulfide-isomerase A3 precursor (disulfide isomerase ER-60; ERp60)	36	2.78	36.11	38.89	22.22
P11021	78 kDa glucose-regulated protein precursor (GRP 78)	36	2.78	47.22	27.78	22.22
P35579	Myosin heavy chain, nonmuscle type A (cellular myosin heavy chain, type A)	36	2.78	41.67	30.56	25.00
Q9Y446	Plakophilin3	35	28.57	28.57	31.43	11.43
Q01469	Fatty acid-binding protein, epidermal (E-FABP; PA-FABP)	34	17.65	32.35	29.41	20.59
Q09666	Neuroblast differentiation associated protein AHNAK (desmoyokin)	31	16.13	32.26	35.48	16.13
P22626	Heterogeneous nuclear ribonucleoproteins A2/B1 (hnRNP A2/hnRNP B1)	30	6.67	36.67	23.33	33.33
P05387	60S acidic ribosomal protein P2	29	24.14	24.14	27.59	24.14
Q14679	Tubulin tyrosine ligase-like protein 4	27	11.11	25.93	40.74	22.22
Q9Y2L5	TRS85 homologue	26	7.69	34.62	30.77	26.92
P61160	Actin-like protein 2 (actin-related protein 2)	26	7.69	38.46	30.77	23.08
P62917	60S ribosomal protein L8	26	19.23	26.92	26.92	26.92
Q14134	Tripartite motif protein 29 (ataxia-telangiectasia group D-associated protein)	26	23.08	34.62	19.23	23.08
P12821	Angiotensin-converting enzyme, somatic isoform precursor (ACE)	25	60.00	8.00	4.00	28.00
P47929	Galectin-7 (Gal-7; HKL-14; PI7; p53-induced protein 1)	24	8.33	66.67	12.50	12.50
P07737	Profilin-1 (profilin I)	24	16.67	20.83	29.17	33.33
P36578	60S ribosomal protein L4 (L1)	23	26.09	8.70	17.39	47.83
P09211	Glutathione *S*-transferase P (GST class-pi; GSTP1-1)	22	4.55	31.82	22.73	40.91
P52272	Heterogeneous nuclear ribonucleoprotein M (hnRNP M)	22	9.09	18.18	22.73	50.00
P07195	L-lactate dehydrogenase B chain (LDH heart subunit; LDH-H)	22	13.64	36.36	13.64	36.36
P48643	T-complex protein 1, epsilon subunit (TCP-1ε; CCT-ε)	21	4.76	42.86	28.57	23.81
P10599	Thioredoxin (ATL-derived factor; ADF)	21	14.29	28.57	38.10	19.05
P06748	Nucleophosmin (NPM; nucleolar phosphoprotein B23)	21	14.29	28.57	14.29	42.86
P11142	Heat shock cognate 71 kDa protein (heat shock 70 kDa protein 8)	20	5.00	30.00	25.00	40.00
P49411	Elongation factor Tu, mitochondrial precursor (EF-Tu; P43)	20	10.00	30.00	25.00	35.00
P14625	Endoplasmin precursor (94 kDa glucose-regulated protein; GRP94)	20	15.00	45.00	20.00	20.00
P05109	Calgranulin A (migration inhibitory factor–related protein 8; MRP-8)	20	35.00	35.00	15.00	15.00
Q6ZUU7	Hypothetical protein FLJ43318	19	26.32	15.79	42.11	15.79
Q9HCY8	S100 calcium-binding protein A14 (S114)	19	36.84	21.05	26.32	15.79
P30044	Peroxiredoxin 5, mitochondrial precursor (Prx-V)	18	5.56	16.67	44.44	33.33
Q14764	Major vault protein (MVP; lung resistance-related protein)	18	5.56	33.33	38.89	22.22
P18206	Vinculin (metavinculin)	18	11.11	50.00	27.78	11.11
Q14574	Desmocollin 3 precursor (desmocollin 4; HT-CP)	18	16.67	22.22	22.22	38.89
P46781	40S ribosomal protein S9	18	16.67	33.33	16.67	33.33

(*Continued on the following page*)

Table 2. Proteins identified in both normal and tumor HNSCC tissues (Cont'd)

Accession	Protein	Peptides (number)	Normal (%)	WD (%)	MD (%)	PD (%)
P62913	60S ribosomal protein L11 (CLL-associated antigen KW-12)	17	5.88	47.06	23.53	23.53
P62899	60S ribosomal protein L31	16	6.25	43.75	18.75	31.25
Q99456	Keratin, type I cytoskeletal 12 (cytokeratin 12; K12; CK 12)	14	7.14	57.14	21.43	14.29
Q02413	Desmoglein 1 precursor (desmosomal glycoprotein 1; DG1; DGI)	14	14.29	35.71	42.86	7.14
P83731	60S ribosomal protein L24 (ribosomal protein L30)	13	7.69	38.46	23.08	30.77
P46940	Ras GTPase-activating-like protein IQGAP1 (p195)	13	7.69	30.77	30.77	30.77
P00505	Aspartate aminotransferase, mitochondrial precursor (transaminase A)	13	15.38	23.08	7.69	53.85
P78371	T-complex protein 1, β subunit (TCP-1-β; CCT-β)	13	15.38	30.77	30.77	23.08
P50990	T-complex protein 1, θ subunit (TCP-1-θ; CCT-θ)	13	23.08	38.46	15.38	23.08
O60506	Heterogeneous nuclear ribonucleoprotein Q (hnRNP Q)	12	8.33	41.67	41.67	8.33
Q00610	Clathrin heavy chain 1 (CLH-17)	12	16.67	33.33	8.33	41.67
O60437	Periplakin (195 kDa cornified envelope precursor protein)	12	25.00	25.00	25.00	25.00
Q07020	60S ribosomal protein L18	12	33.33	33.33	25.00	8.33
P30041	Peroxiredoxin 6 (antioxidant protein 2)	11	18.18	18.18	27.27	36.36
Q96AA2	Obscurin	11	18.18	36.36	27.27	18.18
Q5U4P6	KHSRP protein	11	18.18	45.45	9.09	27.27
Q08881	Tyrosine-protein kinase ITK/TSK	11	18.18	36.36	27.27	18.18
P13639	Elongation factor 2 (EF-2)	11	27.27	45.45	9.09	18.18
P35321	Cornifin A (small proline-rich protein IA; SPR-IA; SPRK)	11	27.27	45.45	9.09	18.18
P22528	Cornifin B (small proline-rich protein IB; SPR-IB)	11	36.36	36.36	9.09	18.18
Q01518	Adenylyl cyclase-associated protein 1 (CAP 1)	10	10.00	30.00	20.00	40.00
P08572	Collagen α 2(IV) chain precursor	10	10.00	50.00	20.00	20.00
Q96MG1	Hypothetical protein FLJ32421	10	10.00	50.00	30.00	10.00
O75312	Zinc-finger protein ZPR1 (zinc finger protein 259)	10	30.00	10.00	10.00	50.00
Q8TBA0	Chromosome 8 open reading frame 21	10	30.00	20.00	10.00	40.00
Q96CN5	Hypothetical protein MGC20806	10	30.00	40.00	10.00	20.00
P40121	Macrophage capping protein (actin-regulatory protein CAP-G)	9	11.11	11.11	44.44	33.33
P06733	α Enolase (Enolase 1)	9	11.11	22.22	33.33	33.33
P12035	Keratin, type II cytoskeletal 3 (cytokeratin 3; K3)	9	11.11	44.44	22.22	22.22
O00299	Chloride intracellular channel protein 1 (nuclear chloride ion channel 27)	9	11.11	44.44	22.22	22.22
Q02388	Collagen α 1(VII) chain precursor (long-chain collagen; LC collagen)	9	22.22	11.11	11.11	55.56
Q9Y6X9	Zinc finger CW-type coiled-coil domain protein 1	9	22.22	55.56	11.11	11.11
P04080	Cystatin B (liver thiol proteinase inhibitor; CPI-B; Stefin B)	9	33.33	33.33	22.22	11.11
P49368	T-complex protein 1, γ subunit (TCP-1-γ; CCT-γ)	8	12.50	12.50	25.00	50.00
Q6ZT17	Hypothetical protein FLJ45043	8	12.50	25.00	25.00	37.50
O15353	Forkhead box protein N1 (transcription factor winged-helix nude)	8	37.50	25.00	25.00	12.50
P28715	DNA excision repair protein ERCC-5	8	50.00	25.00	12.50	12.50
P24534	Elongation factor 1-β (EF-1-β)	7	14.29	14.29	28.57	42.86
Q8N7I6	Hypothetical protein FLJ25506	6	16.67	16.67	33.33	33.33
P62277	40S ribosomal protein S13	6	16.67	16.67	16.67	50.00
Q99551	Transcription termination factor, mitochondrial precursor (mTERF)	6	16.67	33.33	33.33	16.67
P31153	*S*-adenosylmethionine synthetase γ form (AdoMet synthetase)	6	16.67	50.00	16.67	16.67
Q9UKG9	Peroxisomal carnitine *O*-octanoyltransferase (COT)	6	33.33	16.67	33.33	16.67
Q15369	Transcription elongation factor B polypeptide 1 (elongin C)	6	50.00	16.67	16.67	16.67
Q06830	Peroxiredoxin 1 (EC 1.11.1.-; thioredoxin peroxidase 2)	5	20.00	20.00	40.00	20.00
O75151	PHD finger protein 2 (GRC5)	4	25.00	25.00	25.00	25.00
O60231	Putative pre-mRNA splicing factor RNA helicase (DEAH-box protein 16)	4	25.00	25.00	25.00	25.00
P52907	F-actin capping protein α-1 subunit (CapZ α-1)	4	25.00	25.00	25.00	25.00
Q99698	Lysosomal trafficking regulator (Beige homologue)	4	25.00	25.00	25.00	25.00
Q8TBU6	Hypothetical protein FLJ11848	4	25.00	25.00	25.00	25.00

NOTE: Proteins that were identified as common in all normal and HNSCC tissues were sorted across data sets of the different tissue samples as described in Materials and Methods, based on the corresponding peptide number in descending order and their relative distribution (%) across the different samples: normal, WD, MD, and PD HNSCC. Accession number for each protein is also indicated.

(19, 20). Full lists of proteins for these comparisons are available in Supplementary Tables S5 to S7.

Gene ontology analysis. Analysis of each sample set resulted in the identification of a large number of proteins. Therefore, it was necessary to integrate these data based on our currently available knowledge of biological functions to determine their individual biological roles and to recognize categories of proteins that may be underrepresented or overrepresented in tumors. For this, we used bioinformatic tools to classify proteins across each of the HNSCC tumor types into different gene ontology categories. This approach enabled the examination of the overall cellular compartment in which the identified proteins are expected to reside and function. Although a minimal difference was observed between normal and HNSCC samples, we found that 133-295, 10-21, 77-185, and 86-184 proteins were associated with the cytoplasm, extracellular matrix, membrane, and the nucleus, respectively. Analysis of the biological processes in which these proteins act revealed

Table 3. Proteins identified only in tumoral HNSCC tissues

Accession	Protein	Peptides (number)	WD (%)	MD (%)	PD (%)
P08670	Vimentin	79	36.71	44.30	18.99
P02452	Collagen α 1(I) chain precursor	57	43.86	29.82	26.32
P23396	40S ribosomal protein S3	27	59.26	29.63	11.11
Q15365	Poly(rC)-binding protein 1 (α-CP1; hnRNP-E1; nucleic acid binding protein SUB2.3)	25	36.00	36.00	28.00
P23246	Splicing factor, proline-and glutamine-rich (PSF)	23	34.78	21.74	43.48
P06396	Gelsolin precursor (actin-depolymerizing factor; ADF; brevin; AGEL)	23	47.83	30.43	21.74
P67936	Tropomyosin α 4 chain (tropomyosin 4; TM30p1)	22	40.91	31.82	27.27
Q8NFW1	α1 Type XXII collagen	22	31.82	40.91	27.27
P29401	Transketolase (EC 2.2.1.1; TK)	20	50.00	35.00	15.00
Q8NC51	Plasminogen activator inhibitor 1 (PAI1)	19	42.11	42.11	15.79
P07108	Acyl-CoA-binding protein (ACBP; diazepam binding inhibitor, DBI; endozepine, EP)	19	42.11	31.58	26.32
Q96AE4	Far upstream element binding protein 1 (FUSE binding protein 1, FBP)	18	27.78	27.78	44.44
P13796	L-plastin (lymphocyte cytosolic protein 1, LCP-1; LC64P)	17	35.29	35.29	29.41
P22105	Tenascin X precursor (TN-X; hexabrachion-like)	17	41.18	29.41	29.41
O94851	Protein MICAL-2	17	23.53	47.06	29.41
O43707	α-actinin 4 (Nonmuscle α-actinin 4; F-actin cross-linking protein)	16	43.75	18.75	37.50
P26038	Moesin (membrane-organizing extension spike protein)	15	13.33	60.00	26.67
Q9HDC5	Junctophilin 1 (junctophilin type 1, JP-1)	15	20.00	33.33	46.67
P31946	14-3-3 Protein β/α (protein kinase C inhibitor protein-1; KCIP-1; protein 1054)	15	33.33	40.00	26.67
P28065	Proteasome subunit β type 9 precursor (proteasome chain 7; macropain chain 7)	15	46.67	40.00	13.33
Q8N7Z2	Hypothetical protein FLJ40198	15	40.00	33.33	26.67
P07237	Protein disulfide-isomerase precursor (PDI)	15	46.67	26.67	26.67
P00354	Glyceraldehyde-3-phosphate dehydrogenase, muscle (EC 1.2.1.12; GAPDH)	14	42.86	28.57	28.57
Q9P2E9	Ribosome-binding protein 1 (ribosome receptor protein)	14	42.86	35.71	21.43
P02461	Collagen α 1(III) chain precursor	14	28.57	42.86	28.57
P42224	Signal transducer and activator of transcription 1-α/β	14	57.14	28.57	14.29
Q9BVC6	Hypothetical protein MGC5508	13	23.08	30.77	46.15
P05783	Keratin, type I cytoskeletal 18 (cytokeratin 18; K18; CK 18)	13	23.08	15.38	61.54
P22314	Ubiquitin-activating enzyme E1 (A1S9 protein)	13	53.85	23.08	23.08
P07339	Cathepsin D precursor (EC 3.4.23.5)	13	61.54	23.08	15.38
P00338	L-Lactate dehydrogenase A chain (EC 1.1.1.27; LDH-A; LDH muscle subunit; LDH-M)	13	69.23	15.38	15.38
Q99623	B-cell receptor-associated protein BAP37 (D-prohibitin)	12	33.33	16.67	50.00
P06703	Calcyclin (prolactin receptor associated protein, PRA)	12	66.67	25.00	8.33
P11166	Solute carrier family 2, facilitated glucose transporter, member 1	11	27.27	27.27	45.45
P31146	Coronin-1A (coronin-like protein p57; coronin-like protein A)	11	27.27	45.45	27.27
P04179	Superoxide dismutase [Mn], mitochondrial precursor (EC 1.15.1.1)	10	20.00	30.00	50.00
O15083	ERC protein 2	10	30.00	30.00	40.00
Q9NZM4	Glioma tumor suppressor candidate region gene 1 protein	10	30.00	30.00	40.00
P52565	Rho GDP-dissociation inhibitor 1 (Rho GDI 1; Rho-GDI α)	10	30.00	50.00	20.00
P62851	40S ribosomal protein S25	10	40.00	40.00	20.00
Q9BPX3	Condensin subunit 3 (chromosome-associated protein G; NY-MEL-3 antigen)	10	50.00	20.00	30.00
P20908	Collagen α 1(V) chain precursor	10	50.00	30.00	20.00
Q9Y6R0	Numb-like protein (Numb-R)	9	22.22	44.44	33.33
P55786	Puromycin-sensitive aminopeptidase (EC 3.4.11.-; PSA)	9	33.33	22.22	44.44
P26641	Elongation factor 1-γ (EF-1-γ; eEF-1B γ; PRO1608)	9	44.44	11.11	44.44
P40926	Malate dehydrogenase, mitochondrial precursor (EC 1.1.1.37)	9	44.44	22.22	33.33
P20700	Lamin B1	9	44.44	33.33	22.22
Q8WY91	THAP domain protein 4 (PP238; CGI-36)	8	25.00	25.00	50.00
Q9NZT1	Calmodulin-like protein 5 (calmodulin-like skin protein)	8	50.00	25.00	25.00
P08195	4F2 cell-surface antigen heavy chain (4F2hc; CD98 antigen)	8	37.50	37.50	25.00
P27797	Calreticulin precursor (CRP55; calregulin; HACBP; ERp60; grp60)	8	50.00	12.50	37.50
P23368	NAD-dependent malic enzyme, mitochondrial precursor (malic enzyme 2)	8	62.50	12.50	25.00
P27348	14-3-3 protein τ (14-3-3 protein θ; 14-3-3 protein T-cell; HS1 protein)	7	28.57	42.86	28.57
P14314	Glucosidase II β subunit precursor (PKCSH)	7	28.57	57.14	14.29
Q02487	Desmocollin 2A/2B precursor (desmosomal glycoprotein II and III; desmocollin-3)	7	42.86	28.57	28.57
Q01105	SET protein (phosphatase 2A inhibitor I2PP2A; I-2PP2A; template activating factor I)	7	42.86	42.86	14.29
P05023	Sodium/potassium-transporting ATPase α-1 chain precursor (sodium pump 1)	7	28.57	42.86	28.57
P32119	Peroxiredoxin 2 (thioredoxin peroxidase 1; natural killer cell enhancing factor B)	7	42.86	28.57	28.57
Q6ZRH9	Hypothetical protein FLJ46347	7	42.86	42.86	14.29
P27824	Calnexin precursor (MHC class I antigen-binding protein p88)	7	42.86	14.29	42.86
Q9Y2G4	Ankyrin repeat domain protein 6	7	42.86	28.57	28.57
Q9P2H1	KIAA1376 protein (fragment)	7	42.86	42.86	14.29
Q6UVZ0	GLSR2492	7	57.14	28.57	14.29
Q96LT0	Hypothetical protein FLJ25091	7	57.14	14.29	28.57
P18827	Syndecan-1 precursor (SYND1; CD138 antigen)	7	71.43	14.29	14.29

(*Continued on the following page*)

Table 3. Proteins identified only in tumoral HNSCC tissues (Cont'd)

Accession	Protein	Peptides (number)	WD (%)	MD (%)	PD (%)
P62829	60S ribosomal protein L23 (ribosomal protein L17)	7	57.14	28.57	14.29
P61088	Ubiquitin-conjugating enzyme E2 N (ubiquitin-protein ligase N)	7	42.86	28.57	28.57
P84098	60S ribosomal protein L19	7	71.43	14.29	14.29
P05164	Myeloperoxidase precursor (EC 1.11.1.7; MPO)	7	71.43	14.29	14.29
P62258	14-3-3 protein epsilon (14-3-3E)	6	16.67	66.67	16.67
Q6ZVR1	Hypothetical protein FLJ42200	6	16.67	66.67	16.67
P37290	IFN δ-1 precursor	6	16.67	50.00	33.33
Q5VVY7	OTTHUMP00000040479	6	50.00	33.33	16.67
O75874	Isocitrate dehydrogenase [NADP] cytoplasmic (oxalosuccinate decarboxylase)	6	33.33	16.67	50.00
Q12931	Heat shock protein 75 kDa, mitochondrial precursor (HSP 75; TRAP-1)	6	33.33	33.33	33.33
P20794	Serine/threonine-protein kinase MAK (male germ cell-associated kinase)	6	33.33	50.00	16.67
Q99797	Mitochondrial intermediate peptidase, mitochondrial precursor (MIP)	6	50.00	16.67	33.33
Q96RJ0	Trace amine receptor 1 (TaR-1)	6	66.67	16.67	16.67
P61026	Ras-related protein Rab-10	6	50.00	16.67	33.33
Q16401	26S proteasome non-ATPase regulatory subunit 5 (26S proteasome subunit S5B)	6	50.00	33.33	16.67
Q9NXG7	Hypothetical protein FLJ20261	5	20.00	20.00	60.00
Q15717	ELAV-like protein 1 (Hu-antigen R; HuR)	5	40.00	20.00	40.00
P35232	Prohibitin	5	20.00	20.00	60.00
P12532	Creatine kinase, ubiquitous mitochondrial precursor (U-MtCK)	5	20.00	60.00	20.00
Q6IQ21	Hypothetical protein FLJ20582	5	40.00	40.00	20.00
Q8N442	Hypothetical protein FLJ13220	5	40.00	40.00	20.00
Q96GY3	Protein F25965	5	40.00	20.00	40.00
Q13029	PR-domain zinc finger protein 2 (retinoblastoma protein-interacting zinc-finger protein)	5	40.00	20.00	40.00
Q13442	28 kDa heat- and acid-stable phosphoprotein (PDGF-associated protein)	5	40.00	40.00	20.00
Q9UHD9	Ubiquilin 2 (protein linking IAP with cytoskeleton-2; hPLIC-2)	5	40.00	40.00	20.00
P82914	28S ribosomal protein S15, mitochondrial precursor (S15mt; MRP-S15; DC37)	5	60.00	20.00	20.00
O95571	HSCO protein (ETHE1 protein)	5	60.00	20.00	20.00
Q9H8N1	Hypothetical protein FLJ13385	4	25.00	25.00	50.00
Q6P3R8	MGC75495 protein (OTTHUMP00000040896)	4	25.00	25.00	50.00
P16401	Histone H1.5 (histone H1a)	4	25.00	50.00	25.00
Q8WXX7	Autism susceptibility gene 2 protein	4	25.00	50.00	25.00
Q9UIG0	Bromodomain adjacent to zinc finger domain protein 1B (hWALP2)	4	50.00	25.00	25.00
Q86VX5	SLC25A28 protein (fragment)	4	50.00	25.00	25.00
Q9UHD8	Septin 9 (MLL septin-like fusion protein; septin D1)	4	50.00	25.00	25.00
Q13148	TAR DNA-binding protein-43 (TDP-43)	4	50.00	25.00	25.00
Q13724	Mannosyl-oligosaccharide glucosidase	4	50.00	25.00	25.00
O00303	Eukaryotic translation initiation factor 3 subunit 5 (eIF-3ε)	4	50.00	25.00	25.00
P23381	Tryptophanyl-tRNA synthetase (TrpRS; hWRS)	4	50.00	25.00	25.00
P13804	Electron transfer flavoprotein α-subunit, mitochondrial precursor (α-ETF)	4	50.00	25.00	25.00

NOTE: Proteins identified exclusively in the tumor samples were sorted as described in Materials and Methods based on their peptide number in descending order and their relative distribution (%) across the different samples: WD, MD, and PD.

several groups of molecules that were highly represented in tumors, many involved in cell adhesion, cell cycle, cell differentiation, cellular metabolic process, cell motility, endopeptidase activity, signal transduction, and gene transcription and translation, closely aligned with the processes of carcinogenesis. Indeed, a large number of proteins belonging to these functional groups were ascribed to tumors, and to their normal tissue counterpart, albeit to a lesser extent (Supplementary Table S8). A detailed list of molecules predicted to participate in signal transduction (238 proteins), protein phosphorylation (39 proteins), endopeptidase activity (35 proteins), cell motility (47 proteins), cell cycle regulation (99 proteins), and cell adhesion (71 proteins) across normal tissues and the different tumor phenotypes is provided in Supplementary Tables S9 to S14.

Detection of novel proteins in normal and tumor HNSCC. A key advantage afforded by this proteome-wide analysis is the potential for discovery of new molecules yet to be described for normal and malignant oral squamous tissues. Several hypothetical novel proteins, whose existence is predicated on computational analysis of open reading frames (21), were found to be present in normal and tumor samples. These proteins were collated and organized in descending order based on peptide number. As seen in Supplementary Table S15, the majority of the proteins with ≥4 peptides were detected in either tumor or normal samples. Collectively, the emerging information identified many novel proteins in normal and tumor samples, whose nature can now be analyzed. In this regard, structural features of these previously predicted proteins are quite diverse and suggestive of multiple roles in signal transduction, cell communication, and secretion, among others. Future work could help establish their possible role in HNSCC development and progression.

Proteins identified as of interest for HNSCC. The ability to discriminate subsets of proteins differentially abundant within normal oral squamous epithelia and tumors exhibiting distinct differentiation characteristics provided an opportunity to mine the data to identify proteins of interest as well as putative

biomarkers of HNSCC development and progression. A selected group of molecules identified as being differentially abundant were sorted by total peptide number and their relative distribution across the normal and tumor samples (Table 4). Notably, the peptide distribution of the cytokeratins 14, 17, and 16 was observed to be lower in the normal samples compared with the WD, MD, and PD tumor samples. By contrast, the peptide distribution of cytokeratin 4 was higher in normal (~77%) compared with the tumor samples (~4-12%). Also included in the list are cytokeratins 7 and 18 albeit with a lower peptide number. The relative distribution indicates that these molecules are less abundant in normal samples than in MD and PD tumors, respectively. Molecules involved in cell-to-cell interaction were also identified as potential biomarkers and include desmoplakin, democollin 2A/2B, demoglein 3 precursor, plakophilin 1, and plakophilin 3. The total peptide number for this group of proteins ranged from 7 to 385, with a relative similar distribution in all samples with the exception of democollin 2A/2B, which was undetectable in normal samples. Furthermore, from the total peptide number of 385 for desmoplakin, ~44% of these were detected in well-differentiated tumors and in the other samples indicating close to equal levels. Other proteins of interest include HSP27 and HSP70, vimentin, glutathione *S*-transferase, and integrin β_4. In all these proteins, the distribution of peptides was low to undetectable in normal samples when compared with the tumors. Among the latter, we found proteins that may play a role in tumor progression, such as SET protein (phosphatase 2A inhibitor I2PP2A) and ELAV-like protein 1 (Hu-antigen R), and many surface proteins, including 4F2 cell surface antigen heavy chain (CD98), and, as described above, integrin β_4 (CD104 antigen), which may represent promising markers to study tumor progression.

Validation of biomarkers by immunohistochemistry. Having identified proteins of potential interest to HNSCC progression,

Table 4. Representative proteins of interest for HNSCC

Accession	Protein	Peptides (number)	Normal (%)	WD (%)	MD (%)	PD (%)
P02533	Keratin, type I cytoskeletal 14	449	7.80	42.54	29.18	20.49
P08779	Keratin, type I cytoskeletal 16	387	8.27	41.09	30.23	20.41
P15924	Desmoplakin (DP)	385	15.32	43.90	18.44	22.34
P19013	Keratin, type II cytoskeletal 4	179	77.65	3.91	12.29	6.15
P04264	Keratin, type II cytoskeletal 1	146	18.49	22.60	28.77	30.14
Q13835	Plakophilin 1 (band-6-protein, B6P)	95	16.84	30.53	21.05	31.58
P04792	Heat-shock protein β1 (HspB1; HSP 27)	83	4.82	28.92	31.33	34.94
P08670	Vimentin	79	0.00	36.71	44.30	18.99
Q04695	Keratin, type I cytoskeletal 17	76	6.58	40.79	31.58	21.05
P32926	Desmoglein 3 precursor	65	15.38	29.23	30.77	24.62
P07476	Involucrin	57	8.77	56.14	26.32	8.77
Q9UBC9	Small proline-rich protein 3 (cornifin β)	49	61.22	4.08	6.12	28.57
P11021	78 kDa Glucose-regulated protein (GRP 78)	36	2.78	47.22	27.78	22.22
Q9Y446	Plakophilin 3	35	28.57	28.57	31.43	11.43
P09211	Glutathione *S*-transferase P (GSTP1-1)	22	4.55	31.82	22.73	40.91
P11142	Heat shock cognate 71 kDa protein	20	5.00	30.0	025.00	40.00
Q8NC51	Plasminogen activator inhibitor 1 (PAI1)	19	0.00	42.11	42.11	15.79
Q14764	Major vault protein (MVP)	18	5.56	33.33	38.89	22.22
O43707	α-actinin 4 (nonmuscle α-actinin 4)	16	0.00	43.75	18.75	37.50
P42224	Signal transducer and activator of transcription 1	14	0.00	57.14	28.57	14.29
Q99456	Keratin, type I cytoskeletal 12	14	7.14	57.14	21.43	14.29
P05783	Keratin, type I cytoskeletal 18	13	0.00	23.08	15.38	61.54
P46940	Ras GTPase-activating-like protein IQGAP1 (p195)	13	7.69	30.77	30.77	30.77
P07339	Cathepsin D precursor	13	0.00	61.54	23.08	15.38
P08729	Keratin, type II cytoskeletal 7	11	0.00	0.00	90.90	10.10
P52565	Rho GDP-dissociation inhibitor 1 (Rho GDI 1)	10	0.00	30.00	50.00	20.00
P12821	PIWIL 3 protein	9	88.00	11.00	0.00	0.00
O15353	Forkhead box protein N1	8	37.50	25.00	25.00	12.50
P08195	4F2 cell-surface antigen (CD98)	8	0.00	37.50	37.50	25.00
P28715	DNA excision repair protein ERCC-5	8	50.00	25.00	12.50	12.50
Q02487	Desmocollin 2A/2B precursor (desmocollin-3)	7	0.00	42.86	28.57	28.57
O14757	Serine/threonine-protein kinase Chk1	7	57.00	14.00	0.00	29.00
Q01105	SET protein (phosphatase 2A inhibitor I2PP2A)	7	0.00	42.86	42.86	14.29
Q13015	Protein AF1q	6	0.00	0.00	0.00	100.00
Q15717	ELAV-like protein 1 (Hu-antigen R; HuR)	5	0.0	040.00	20.00	40.00
P35232	Prohibitin	5	0.00	20.00	20.00	60.00
P00533	Epidermal growth factor receptor (EGFR)	4	0.00	50.00	0.00	50.00
Q9UHD8	Septin 9 (MLL septin-like fusion protein)	4	0.00	50.00	25.00	25.00
P16144	Integrin β_4 precursor (CD104)	4	0.00	0.00	25.00	75.00
O43157	Plexin B1 precursor (semaphorin receptor SEP)	3	0.00	33.00	33.00	33.00
O14511	Pro-neuregulin-2 (pro-NRG2)	3	0.00	33.00	33.00	33.00
Q02224	Centromeric protein E (CENP-E protein)	3	0.00	33.00	33.00	33.00

NOTE: Known proteins from the total list that may represent proteins of interest as well as potential biomarkers were sorted based on their total peptide number and relative distribution (%) across the normal and WD, MD, and PD tumor samples.

a subset of these were chosen for validation based on the relative abundance of corresponding peptides in the different samples analyzed. Validation studies were conducted using standard immunohistochemistry in archival HNSCC tissues followed by in-depth analysis of hundreds of HNSCC cases using a recently developed HNSCC-specific TMA. As seen in Fig. 2A, cytokeratin 4 was detected predominantly in the suprabasal layers of the control normal tissues, whereas the expression of this molecule in HNSCC tumors was restricted to only few cells in <20% of WD tumors. Most MD to WD cells stained positive for cytokeratin 16, whereas in the normal tissues this protein was present in the suprabasal layers of the oral squamous epithelium (*second from top*). Desmoplakin (*third from top*) was found to be predominantly membranous, with a higher immunoreactivity in the suprabasal areas of the squamous epithelium in normal tissues. Tumor cells showed intense staining of the membrane together with a moderate to strong cytoplasmic staining, distributed mostly along the more differentiated areas of all the tumor cases examined. Analysis of desmoglein-3 (*fourth from top*) showed sharp staining within the membrane in normal oral squamous mucosa with a stronger signal in suprabasal layers. Desmoglein-3 was also positive in all tumor samples, following a membrane distribution and a less intense cytoplasmic signal. Immunodetection of vimentin (*bottom*) was positive in only a few normal isolated cells with very distinct dendritic-like morphology in the oral squamous epithelium, whereas the underlying stromal cells were all intensely stained. By contrast, a high proportion of the malignant squamous cells in the tumor cases showed increased immunoreactivity to vimentin. Collectively, the data indicate that the profile of protein expression identified using MS is reflected in an independent archival HNSCC sample set.

The previous data indicated that a subset of proteins (cytokeratin 4, cytokeratin 16, vimentin, and desmoplakin) could effectively distinguish the differing differentiation compartments in archival HNSCC tissues. Therefore, we chose to use an oral cancer–specific TMA for the high-throughput staining and scoring of these predictive immunohistochemical markers in this cancer type. As shown in Fig. 2B (*top*), although cytokeratin 4 was poorly expressed in the majority of the tumors (*left* and *inset*), strong staining for cytokeratin 16 in HNSCC was observed almost exclusively in WD tumors or otherwise WD areas (*second from left* and *inset*), as most MD and PD tumors failed to react strongly. Vimentin immunoreactivity was almost exclusively limited to a subset of malignant tumors, and in the majority of the cases this staining was focal (*third from left* and *inset*). Finally, staining for desmoplakin was strongly positive in normal tissues as well as in almost all tumor samples (*right* and *inset*).

A semiquantitative analysis was applied to the TMA staining. As indicated in Fig. 2B (*bottom*), cytokeratin 4 and cytokeratin 16 scored positive in normal tissues based on the staining pattern of the suprabasal layer, and their expression in tumors was often restricted to WD areas. For the evaluation of vimentin (*third from left*) and desmoplakin (*right*), we classified cell staining in each tissue core as positive and negative because no clear correlation with tumor differentiation was noted from the initial analysis. Of note, vimentin and desmoplakin were assessed to be negative and strongly positive, respectively, in all the relevant normal oral epithelial tissues analyzed.

Discussion

In this study, we describe the utility of a novel proteomics platform for the global detection of expressed proteins in FFPE tissues and its use for biomarker discovery and identification of proteins that may contribute to HNSCC development and progression. This approach enabled identification of a large number of molecules, including cytokeratins and intermediate filament proteins, differentiation markers, proteins involved in stem cell maintenance, signal transduction and cell cycle regulation, growth and angiogenic factors, matrix-degrading proteases, and proteins with tumor suppressive and oncogenic potential. Of interest, detection and relative expression of many of these molecules followed a distinct pattern in normal squamous epithelia and WD, MD, and PD HNSCC tumor tissues. The ability to correlate protein expression profiles with histopathologic classification of disease may allow the development of novel biomarkers of diagnostic and prognostic value and may help identify novel targets for therapeutic intervention in HNSCC.

Certain advantages embedded within the workflow developed for this study include the efficient solubilization and digestion of proteins from FFPE archival tissue without fractionation, such that they are amenable for identification using tandem MS for a complete proteomic representation (7). Furthermore, optimization of combining laser capture microdissection with shotgun proteomic technologies enabled the detection of proteins expressed primarily within the tumor cells rather than in the stroma and other complex cellular components of the tumor microenvironment. Although the exactness of MS identifications can be challenging, particularly for low abundant proteins, current MS instrumentation and improved bioinformatic capabilities provide a high probability of protein identification (22). Thus, rather than reporting proteins identified by two or more unique peptide sequence matches, a common practice in the field that may sacrifice many correct protein identifications derived from high-quality single hits, we chose to report here all proteins identified based on stringent biophysical and statistical criteria. Indeed, the ability to take advantage of new technological developments may now enable the discovery of molecules that although present in low abundance may nevertheless play important biological roles in tumor development.

In this regard, it was encouraging that certain proteins indicative of "proof of principle" could be readily detected. For example, the total peptide number for glyceraldehyde-3-phosphate dehydrogenase, a protein frequently used for normalization, was nearly equally distributed across the different samples, suggesting that the protein recovery was similar for each group of tissues. Further validation of our analysis was illustrated by the identification of members of the taste receptors (T2R13, T2R38), olfactory receptors (5M11, 13C4, JCG2), and oral facial proteins (oral-facial-digital syndrome 1 protein), each with a single peptide. Although these proteins may not be involved in cancer, they are nevertheless known to be expressed in oral squamous tissues (23–25). The abundance of the cytokeratins (1, 4, 5, 7, 14, 16–18) and the desmosomal proteins (desmoplakin, desmoglein 3, desmocollin, epiplakin, plakophilins) was striking, particularly when considering the limited amount of sample available for the proteomic analysis. Noteworthy, desmoglein 1

and desmoglein 3 are both expressed in the skin, but the 130 kDa molecule desmoglein 3 is preferentially expressed in oral epithelium (26). As these molecules function together to maintain structural integrity of the normal oral epithelium, changes in their relative levels might represent putative biomarkers of disease progression (26).

From these long lists of proteins identified in normal and cancer cells, can we find those that may contribute to cancer development? The answer is likely yes, when considering the nature of many of the proteins identified that are predicted to be involved in cell cycle regulation, signal transduction, and proteolysis. For example, checkpoint kinase 1, a serine/threonine protein kinase that is a key mediator in the DNA damage–induced checkpoint network (27), was highly detected in normal epithelia but poorly detected in HNSCC tumors. Similarly, Apc, the protein product of the *adenomatous polyposis coli* (*apc*) gene that prevents aberrant activity of the Wnt/β-catenin signaling system and is the most frequently mutated molecule in colon cancer (28), was detected as a single peptide only in normal oral epithelium. Low-density lipoprotein receptor–related protein 12, also known as suppressor of tumorigenicity protein 7, a tumor suppressive protein whose gene is located on human chromosome 8 q22.2-23.1, a locus of high polymorphism and genetic alterations in cancer biopsies including HNSCC (29), was only found in normal oral epithelium. Similarly, a single peptide for cyclin K, a protein that acts as a regulatory subunit of CDK9 thereby regulating the transcription of a subset of genes (30), was detected only in normal tissues. As cyclin K is regulated by p53, its loss in tumor tissues may reflect the decreased p53 activity that characterizes HNSCC (3). Aligned with this possibility, individual peptides for a tumor suppressor gene on 17p13.3, *hypermethylated in cancer 1*, *HIC-1*, and a direct target for p53 that is involved in the inhibition of cell growth and the initiation of cell death and senescence programs in response to DNA damage (31), were identified in normal epithelial cells but only in one case of PD tumor sample. Thus, a DNA damage sensing molecule, checkpoint kinase 1, at least two p53 targets, cyclin K and HIC-1, as well as lipoprotein receptor–related protein 12 and Apc, the latter a well-known tumor suppressor protein poorly investigated in HNSCC, seem to be more prominent in normal epithelial than in tumor cells. Collectively, these results suggest the existence of a network of tumor-restricting mechanisms that protect the integrity of the normal squamous epithelium whose loss or decreased expression and function may contribute to HNSCC progression.

On the other hand, several proteins involved in cell cycle progression, particularly G_2-M transition and mitosis, such as septin 9 and centromeric protein E, were only detected in tumor samples, reflecting their active state of proliferation. An unusual cell cycle regulating protein, prohibitin, which has been recently observed to play an unexpected function in the activation of Raf/MEK/ERK pathway by Ras and in modulating epithelial cell adhesion and migration (32), was only detected in tumors. Another surprising finding was the detection of two peptides derived from *EVI-5* oncogene. This protein was first identified in experimental T-cell lymphomas by retroviral insertion strategies and has been recently shown to act together with Polo-like kinase to ensure mitotic fidelity (33). Thus, both prohibitin and EVI-5 may represent excellent candidates to play a role in aberrant cell growth in HNSCC.

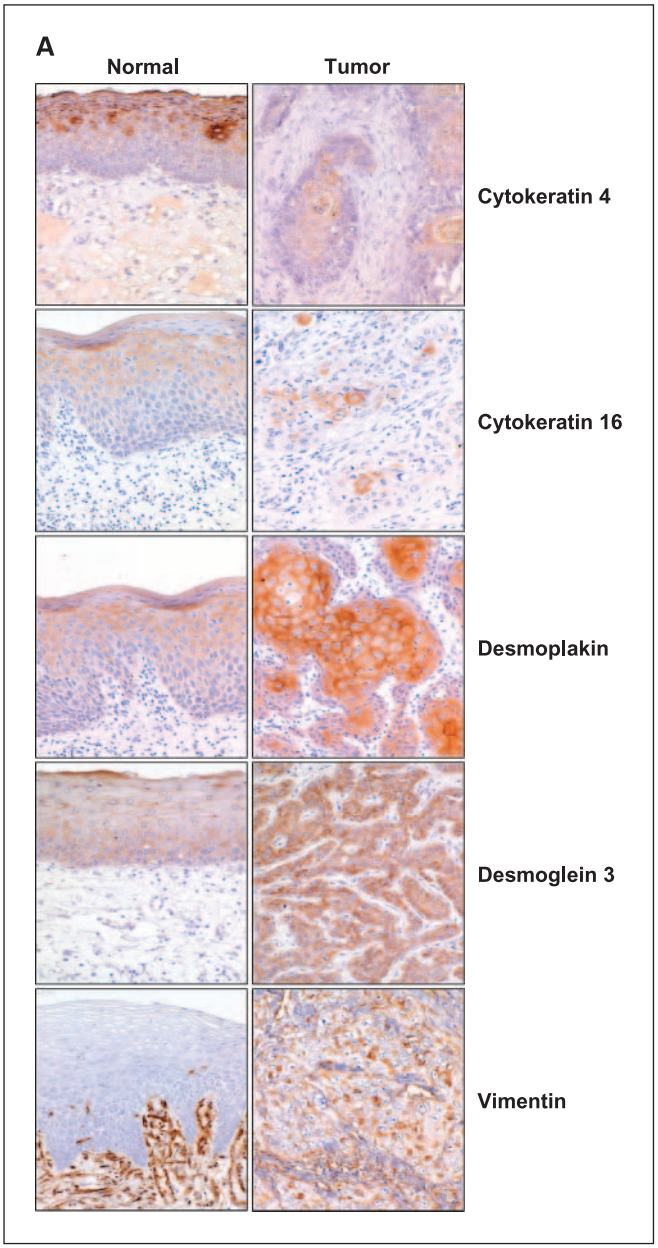

Fig. 2. Validation of biomarkers by immunohistochemistry on archival HNSCC tissues. *A,* archival tissues consisting normal and tumor HNSCC were processed and used for immunodetection of the indicated proteins with appropriate antibodies as described in Materials and Methods.

Several molecules with a role in the transduction of proliferative signals were also identified in normal and tumor HNSCC cells. For example, epidermal growth factor receptor was detected in tumor samples but not in normal oral epithelial tissues, reflecting the overexpression of this growth factor tyrosine kinase receptor in HNSCC (34). We also found expression of one epidermal growth factor receptor ligand, neuregulin-2, in HNSCC, suggesting an increased complexity of the epidermal growth factor receptor network in squamous carcinogenesis. Similarly, numerous signaling molecules involved in cell migration were detected in HNSCC cells. They include several members of the Rho family of small GTPases, and few peptides derived from two novel guanine nucleotide

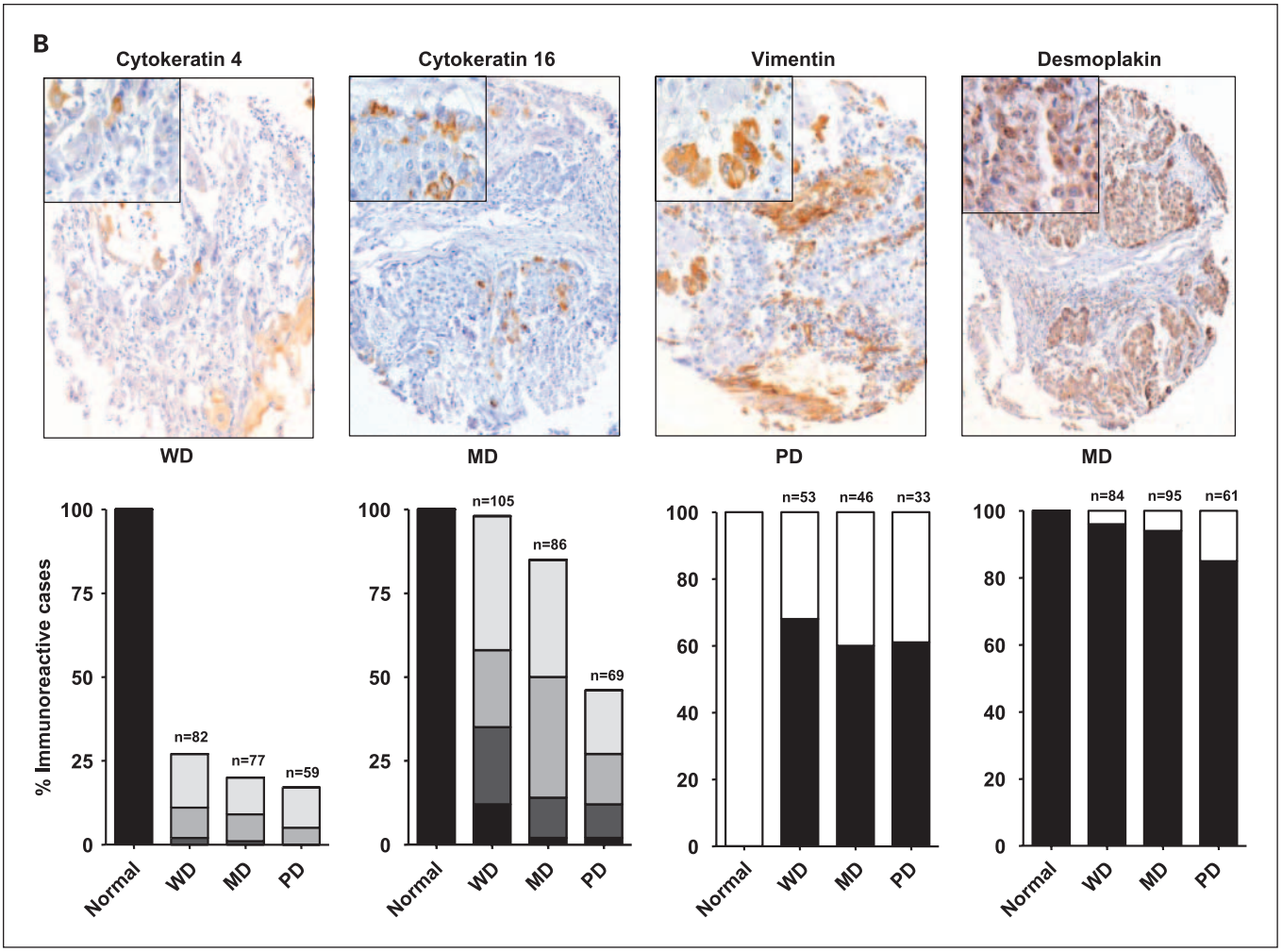

Fig. 2 *Continued*. *B,* analysis of HNSCC biomarkers in HNSCC-specific TMA. Head and neck – specific TMAs consisting of control and WD, MD, and PD HNSCC tumor samples were stained for indicated proteins with appropriate antibodies as described in Materials and Methods. Representative TMA cores are depicted (*top*). Stained TMAs were "scored" based on tissue differentiation and staining intensity. For cytokeratin 4 and cytokeratin 16, light gray represents ›5% and ‹25% of cells stained; mid gray, 26% to 50% of the cells stained; dark gray, 51% to 75%; and black, 76% to 100% of the cells stained. For vimentin and desmoplakin, the percentage of positive tumors for each stage of differentiation (*black box*) compared with negative (*white box*) is depicted. In each case, the number of nonneoplastic (*Normal*) tissues analyzed was 10, and the number of HNSCC cancer tissues is indicated.

exchange factors for Rho GTPases, RhoGEF 10 and RhoGEF 19, in tumor cells, all suggestive of an important role for Rho GTPases and their regulatory proteins and downstream targets in HNSCC progression. Two cell surface receptors, integrin β_4 and plexin B1, which are involved in cell motility were also readily detected in tumor cells. In this regard, whereas integrin β_4 contributes to keratinocyte cell migration and facilitates tumor angiogenesis (35), plexin B1, which was initially identified based on its role in axons guidance, is now known to play an important role in endothelial cell migration and tumor angiogenesis (36). We have also shown that HNSCC express high levels of the plexin B1 ligand, semaphorin 4D (37), suggesting the existence of an autocrine plexin B1–semaphorin 4D loop that may promote HNSCC cell migration. These proteins may also promote aberrant HNSCC growth, as suggested by recent studies indicating that integrin β_4 and plexin B1 can stimulate members of the epidermal growth factor receptor and Met family of growth factor receptors (38–40).

Proteases and their inhibitors form a complex proteolytic system and are ultimately responsible for cancer cell invasion and metastasis. In this study, the abundance of members of the ADAMTS proteases family was particularly notable. These proteases likely contribute to extracellular matrix degradation, cell-to-cell adhesion, cell proliferation, and migration, and the processing of cytokines and growth factors, all aiding tumor progression and angiogenesis. Cathepsin D, which is a lysosomal aspartic protease, was also detected in the samples. Although cathepsins are involved in bulk protein turnover, they also have specialized roles in processes such as growth factor turnover and antigen presentation (41, 42). Cathepsin D was the most detectable protease in HNSCC samples, particularly in MD tumor cells. This cathepsin is often observed to be largely overexpressed in breast cancer tissues and their derived cell lines and its expression levels correlate with the incidence of clinical metastasis and shorter survival times (43). Furthermore, cathepsin D overexpression increases the growth and metastatic potential of different cancer cells *in vivo* (43). Thus, emerging

evidence and our present findings suggest that this protease may play an unsuspected role in HNSCC progression.

Taken together, the ability to combine laser capture microdissection and in-depth proteomic analysis of formalin-fixed, paraffin-embedded tissues provides a wealth of information regarding the nature of the proteins expressed in normal squamous epithelium and tumor progression. These proteins include a number of tumor suppressor molecules and microRNA processing proteins likely involved in protecting the integrity of the cellular genome in normal epithelial cells and their resident progenitor stem cells, as well as many molecules involved in aberrant cell proliferation, survival, angiogenesis, proteolysis, and migration, whose contribution to tumor growth, resistance to treatment, and the metastatic spread of HNSCC can now begin to be explored. The emerging information has also enabled identification of a large number of proteins that are differentially expressed in normal oral squamous epithelia and tumors exhibiting distinct differentiation characteristics, thus representing suitable makers to study tumor progression. The future evaluation of the tumor makers described in this study may afford an opportunity to explore their diagnostic and prognostic value, in particular for the early detection of HNSCC. On the other hand, we expect that our study, documenting the successful use of proteomic techniques and bioinformatic tools to analyze molecules expressed in archival tumor and normal tissues, may now provide a proof of principle that will boost ongoing systems to increase the scale of data-generating proteomic efforts, which may ultimately lead to discovery of novel clinically relevant biomarkers and therapeutic targets for HNSCC and other human malignancies.

Acknowledgments

We thank Thomas H. Bugge, Ana Raimondi, Panomwat Amornphimoltham, Chidchanok Leethanakul, Robert T. Dorsam, Thomas Guiel, and Marlene Darfler for their technical help, advice, and guidance.

References

1. Jemal A, Siegel R, Ward E, et al. Cancer statistics, 2007. CA Cancer J Clin 2007;57:43–66.
2. Mao L, Hong WK, Papadimitrakopoulou VA. Focus on head and neck cancer. Cancer Cell 2004;5:311–6.
3. Forastiere A, Koch W, Trotti A, Sidransky D. Head and neck cancer. N Engl J Med 2001;345:1890–900.
4. Nguyen DX, Massague J. Genetic determinants of cancer metastasis. Nat Rev Genet 2007;8:341–52.
5. Nagaraja GM, Othman M, Fox BP, et al. Gene expression signatures and biomarkers of noninvasive and invasive breast cancer cells: comprehensive profiles by representational difference analysis, microarrays and proteomics. Oncogene 2006;25:2328–38.
6. Wulfkuhle JD, Liotta LA, Petricoin EF. Proteomic applications for the early detection of cancer. Nat Rev Cancer 2003;3:267–75.
7. Canas B, Pineiro C, Calvo E, et al. Trends in sample preparation for classical and second generation proteomics. J Chromatogr A 2007;1152:235–58.
8. Fermin D, Allen BB, Blackwell TW, et al. Novel gene and gene model detection using a whole genome open reading frame analysis in proteomics. Genome Biol 2006;7:R35.
9. Umar A, Luider TM, Foekens JA, Pasa-Tolic L. NanoLC-FT-ICR MS improves proteome coverage attainable for approximately 3000 laser-microdissected breast carcinoma cells. Proteomics 2007;7:323–9.
10. Baker H, Patel V, Molinolo AA, et al. Proteome-wide analysis of head and neck squamous cell carcinomas using laser-capture microdissection and tandem mass spectrometry. Oral Oncol 2005;41:183–99.
11. Ahram M, Flaig MJ, Gillespie JW, et al. Evaluation of ethanol-fixed, paraffin-embedded tissues for proteomic applications. Proteomics 2003;3:413–21.
12. Molinolo AA, Hewitt SM, Amornphimoltham P, et al. Dissecting the Akt/mammalian target of rapamycin signaling network: emerging results from the head and neck cancer tissue array initiative. Clin Cancer Res 2007;13:4964–73.
13. Hood BL, Darfler MM, Guiel TG, et al. Proteomic analysis of formalin-fixed prostate cancer tissue. Mol Cell Proteomics 2005;4:1741–53.
14. Ashburner M, Ball CA, Blake JA, et al.; The Gene Ontology Consortium. Gene ontology: tool for the unification of biology. Nat Genet 2000;25:25–9.
15. Lo WY, Tsai MH, Tsai Y, et al. Identification of overexpressed proteins in oral squamous cell carcinoma (OSCC) patients by clinical proteomic analysis. Clin Chim Acta 2007;376:101–7.
16. Kaur J, Srivastava A, Ralhan R. Expression of 70-kDa heat shock protein in oral lesions: marker of biological stress or pathogenicity. Oral Oncol 1998;34:496–501.
17. Li DQ, Hou YF, Wu J, et al. Gene expression profile analysis of an isogenic tumour metastasis model reveals a functional role for oncogene AF1Q in breast cancer metastasis. Eur J Cancer 2006;42:3274–86.
18. Sasaki T, Shiohama A, Minoshima S, Shimizu N. Identification of eight members of the Argonaute family in the human genome small star, filled. Genomics 2003;82:323–30.
19. Leeman RJ, Lui VW, Grandis JR. STAT3 as a therapeutic target in head and neck cancer. Expert Opin Biol Ther 2006;6:231–41.
20. Amornphimoltham P, Patel V, Sodhi A, et al. Mammalian target of rapamycin, a molecular target in squamous cell carcinomas of the head and neck. Cancer Res 2005;65:9953–61.
21. Nakajima D, Okazaki N, Yamakawa H, et al. Construction of expression-ready cDNA clones for KIAA genes: manual curation of 330 KIAA cDNA clones. DNA Res 2002;9:99–106.
22. Elias JE, Haas W, Faherty BK, Gygi SP. Comparative evaluation of mass spectrometry platforms used in large-scale proteomics investigations. Nat Methods 2005;2:667–75.
23. Chandrashekar J, Mueller KL, Hoon MA, et al. T2Rs function as bitter taste receptors. Cell 2000;100:703–11.
24. Gaudin JC, Breuils L, Haertle T. Mouse orthologs of human olfactory-like receptors expressed in the tongue. Gene 2006;381:42–8.
25. Romio L, Wright V, Price K, et al. OFD1, the gene mutated in oral-facial-digital syndrome type 1, is expressed in the metanephros and in human embryonic renal mesenchymal cells. J Am Soc Nephrol 2003;14:680–9.
26. Chen YJ, Chang JT, Lee L, et al. DSG3 is overexpressed in head neck cancer and is a potential molecular target for inhibition of oncogenesis. Oncogene 2007;26:467–76.
27. Bartek J, Lukas J. Chk1 and Chk2 kinases in checkpoint control and cancer. Cancer Cell 2003;3:421–9.
28. Powell SM, Zilz N, Beazer-Barclay Y, et al. APC mutations occur early during colorectal tumorigenesis. Nature 1992;359:235–7.
29. Garnis C, Coe BP, Zhang L, et al. Overexpression of LRP12, a gene contained within an 8q22 amplicon identified by high-resolution array CGH analysis of oral squamous cell carcinomas. Oncogene 2004;23:2582–6.
30. Baek K, Brown RS, Birrane G, Ladias JA. Crystal structure of human cyclin K, a positive regulator of cyclin-dependent kinase 9. J Mol Biol 2007;366:563–73.
31. Wales MM, Biel MA, el Deiry W, et al. p53 activates expression of HIC-1, a new candidate tumour suppressor gene on 17p13.3. Nat Med 1995;1:570–7.
32. Rajalingam K, Wunder C, Brinkmann V, et al. Prohibitin is required for Ras-induced Raf-MEK-ERK activation and epithelial cell migration. Nat Cell Biol 2005;7:837–43.
33. Eldridge AG, Loktev AV, Hansen DV, et al. The evi5 oncogene regulates cyclin accumulation by stabilizing the anaphase-promoting complex inhibitor emi1. Cell 2006;124:367–80.
34. Kalyankrishna S, Grandis JR. Epidermal growth factor receptor biology in head and neck cancer. J Clin Oncol 2006;24:2666–72.
35. Sehgal BU, DeBiase PJ, Matzno S, et al. Integrin β_4 regulates migratory behavior of keratinocytes by determining laminin-332 organization. J Biol Chem 2006;281:35487–98.
36. Basile JR, Afkhami T, Gutkind JS. Semaphorin 4D/plexin-B1 induces endothelial cell migration through the activation of PYK2, Src, and the phosphatidylinositol 3-kinase-Akt pathway. Mol Cell Biol 2005;25:6889–98.
37. Basile JR, Castilho RM, Williams VP, Gutkind JS. Semaphorin 4D provides a link between axon guidance processes and tumor-induced angiogenesis. Proc Natl Acad Sci U S A 2006;103:9017–22.
38. Bertotti A, Comoglio PM, Trusolino L. β_4 Integrin is a transforming molecule that unleashes Met tyrosine kinase tumorigenesis. Cancer Res 2005;65:10674–9.
39. Giordano S, Corso S, Conrotto P, et al. The semaphorin 4D receptor controls invasive growth by coupling with Met. Nat Cell Biol 2002;4:720–4.
40. Swiercz JM, Kuner R, Offermanns S. Plexin-B1/RhoGEF-mediated RhoA activation involves the receptor tyrosine kinase ErbB-2. J Cell Biol 2004;165:869–80.
41. Reinheckel T, Hagemann S, Dollwet-Mack S, et al. The lysosomal cysteine protease cathepsin L regulates keratinocyte proliferation by control of growth factor recycling. J Cell Sci 2005;118:3387–95.
42. Honey K, Rudensky AY. Lysosomal cysteine proteases regulate antigen presentation. Nat Rev Immunol 2003;3:472–82.
43. Liaudet-Coopman E, Beaujouin M, Derocq D, et al. Cathepsin D: newly discovered functions of a long-standing aspartic protease in cancer and apoptosis. Cancer Lett 2006;237:167–79.

Clinical Cancer Research

Proteomic Analysis of Laser-Captured Paraffin-Embedded Tissues: A Molecular Portrait of Head and Neck Cancer Progression

Vyomesh Patel, Brian L. Hood, Alfredo A. Molinolo, et al.

Clin Cancer Res 2008;14:1002-1014.